



Watershed prioritization in order to implement soil and water conservation practices

Moghadaseh Fallah¹ · Ataollah Kavian² · Ebrahim Omidvar³

Received: 21 March 2016 / Accepted: 31 August 2016
© Springer-Verlag Berlin Heidelberg 2016

Abstract The purpose of this study is to identify erosion-prone in the sub-watersheds of Haraz based on water and soil conservation projects using multi-criteria evaluation method and RS and GIS techniques. In this research, 16 sub-criteria data layers included rainfall erosivity, soil erodibility, land cover, land use, leaf area index, rainfall interception, soil infiltration, slope length, slope gradient, elevation, aspect, bifurcation ratio, basin circularity, length of overland flow, drainage density, drainage texture and form factor were prepared as raster layers. The Revised Universal Soil Loss Equation (RUSLE) was provisioned to predict soil loss ($\text{ton ha}^{-1} \text{ year}^{-1}$) using six factors. Then, sub-criteria were rated based on the soil loss amount of RUSLE map by cutting of sub-criteria maps on RUSLE map, and also original criteria (topography, morphometric, soil, vegetation cover and climate) was weighted by AHP method. The final map was prepared from the multiplication of the weight by rate and in combination with layers in ArcGIS software by the overlay index method. The results showed soil erosion risk index varies from 2.37 to 3.89 in the basin area, and average and standard deviation are 3.06 and 0.28, respectively. Finally, prioritization of sub-watersheds was done based on average weighted of 13 sub-watershed to water and soil conservation practices and was

classified into three priority high, medium and low classes. Five sub-watersheds SW1, SW5, SW8, SW11 and SW3 with total area of 30.52 % had low priority, six sub-watersheds SW4, SW6, SW12, SW13, SW9 and SW7 with total area of 62 % had medium priority, and two sub-watersheds WS2 and WS10 with total area of 7.48 % had high priority. The sub-watersheds under high erosion risk require immediate plans for soil and water conservation practices.

Keywords Prioritization of sub-watersheds · Water and soil conservation · RS · GIS · Haraz watershed

Introduction

Soil erosion by water is the most important problem worldwide, after climate change (Eswaran et al. 2001; Lal 2001; Terranova et al. 2009). Soil erosion creates high economic costs and strong environmental impacts by its effect on water quality, agricultural production and infrastructure (Pimentel et al. 1995; Lal 1998). Assessment of soil erosion hazard at watershed requires mapping and analysis of many factors (Vrieling 2006; Poesen et al. 1996). The soil erosion caused by water is considered the loss of surface soil that caused by rain and runoff, and its amount is measured by the amount of soil loss in a year (Zhang et al. 2010).

There are various model-based methods (ranging from empirical to physically based models) for soil erosion spatial assessment, and quantification of soil loss can be found in (Ni and Li 2003; Lee 2004; Rahman et al. 2009; Zhang et al. 2009; Kim et al. 2012; Alexakis et al. 2013). Each model or approach has its own characteristics and purpose of application (Farhan and Nawaiseh 2015). One

✉ Ataollah Kavian
a.kavian@sanru.ac.ir; ataollah.kavian@yahoo.com

¹ College of Natural Resources, Sari Agricultural Sciences and Natural Resources University, Sari, Iran

² College of Natural Resources, Sari Agricultural Sciences and Natural Resources University, PO. Box 737, Sari, Iran

³ Faculty of Natural Resources and Earth Sciences, University of Kashan, Kashan, Iran

of the most important tools is an analytical hierarchy process (AHP) method (Saaty 1986) with techniques of geographic information system (GIS) and remote sensing (RS). Among major empirical models, the Universal Soil Loss Equation (USLE) (Wischmeier and Smith 1978) is the first and one of the most important of models that is based on experimental data. The model of RUSLE is a revision of the USLE model that has been applied to define erosion hazard in different areas (Terranova et al. 2009). De Steiguer et al. (2003) presented that AHP can be used as a tool for evaluation criteria and identification of best integrated water management plan to watershed conservation. Shri-mali et al. (2001) represented map of prioritizing the regions based on their susceptibility to degradation using RS and GIS technique.

Abdul Rahamana et al. (2015) attempted to study various morphological characteristics and to implement GIS and multi-criteria decision-making (MCDM) through fuzzy analytical hierarchy process (FAHP) techniques for identification of critical sub-watersheds situated in the Kallar watershed, Tamil Nadu. They founded that the FAHP techniques is a practical approach for identification of the sensitive priority zones and is useful for better management practices such as implementation of land and water resource management, conservation and sustainable agricultural development. Zhang et al. (2010) identified conservation priorities by a specific multi-criteria evaluation method. The vegetation cover, land use and slope gradient are used to assess erosion risk in the Yongding river basin, northwest of Beijing city. They founded that the method presented is fast and straightforward, showing good potential for successful application in other areas. By Jaiswal et al. (2014), Saaty's analytical hierarchy process (SAHP) with nine erosion hazards parameters (EHPs) has been used to assess and identify environmentally stressed sub-watersheds in the Benisagar dam catchment of the Bundelkhand region. Eight sub-watersheds and seven sub-watersheds falls were observed under very high and high priority, respectively.

Recent studies represented that RS and GIS techniques are of great use for identification and prioritization of watershed due to estimation of soil loss and other parameters affecting erosion (Jaiswal et al. 2014; Khan et al. 2001; Sharma et al. 2001; Yoshino and Ishioka 2005).

In this context, this study aims to assess and prioritize Haraz sub-watersheds based on soil and water conservation practices. The Haraz watershed is one of the erosion-prone watersheds in Mazandarn, north of Iran country. This study will be applied in the upstream of Haraz dam. This basin is one of the erosion-prone regions due to a geography condition, geostrategic and natural characteristics. According to the erosion-prone and the high sediment potentials in this basin, a large amount of sediment through the main

river are entered into Haraz basin that makes filling the dam reservoir, water pollution and damage to downstream agricultural lands. Therefore, an exact study should be applied in terms of sediment potential in this basin, and then the sub-watersheds are prioritized in order to implement soil and water conservation practices.

Methodology and data

Study area

The study area is the Haraz watershed, located between the north latitude $35^{\circ}45' - 36^{\circ}22'$ and east longitude $51^{\circ}41' - 52^{\circ}36'$ in the northern part of Iran, Mazandaran (Fig. 1). The watershed area is 4014.1 km^2 , and the low and high elevation is 327 and 5671 m above the main sea level (Damavand summit), respectively. The amount of average annual rainfall is about 557.5 mm. The maximum area of the Haraz watershed was covered of pasture and dense brush woods, and in the northeastern from dense and semi-dense forests, there are irrigated land and garden around river, and because of the Alborz mountain in the study area, ridge and rocks are bare areas.

Determination of the sub-watersheds boundary and criteria

The watershed boundaries of the study area were demarcated using SWAT software from the DEM with pixel size of 30 m, and in order to get more accurate management and easier implementation conservation planning in the Haraz watershed, they should be divided into smaller sub-watershed, so the maximum area was given to SWAT software. The drainage basin was extracted using Arc Hydro10 software.

In this study, five main criteria that have the greatest impact on erosion were considered. These criteria including morphometric factors, topography, climate, soil and vegetation cover. For more detailed study of the effective factors on the water erosion, a number of sub-criteria were determined from main criteria. In the present study, AHP has been used for identification of priority sub-watersheds using different criteria that affecting the process of soil erosion in the watersheds. The overall methods used in this study are shown as a flowchart (Fig. 2).

Morphometric

The morphometric characters were divided into two categories linear and shape sub-criteria. The linear sub-criteria such as drainage density, bifurcation ratio, drainage texture and length of overland flow have a

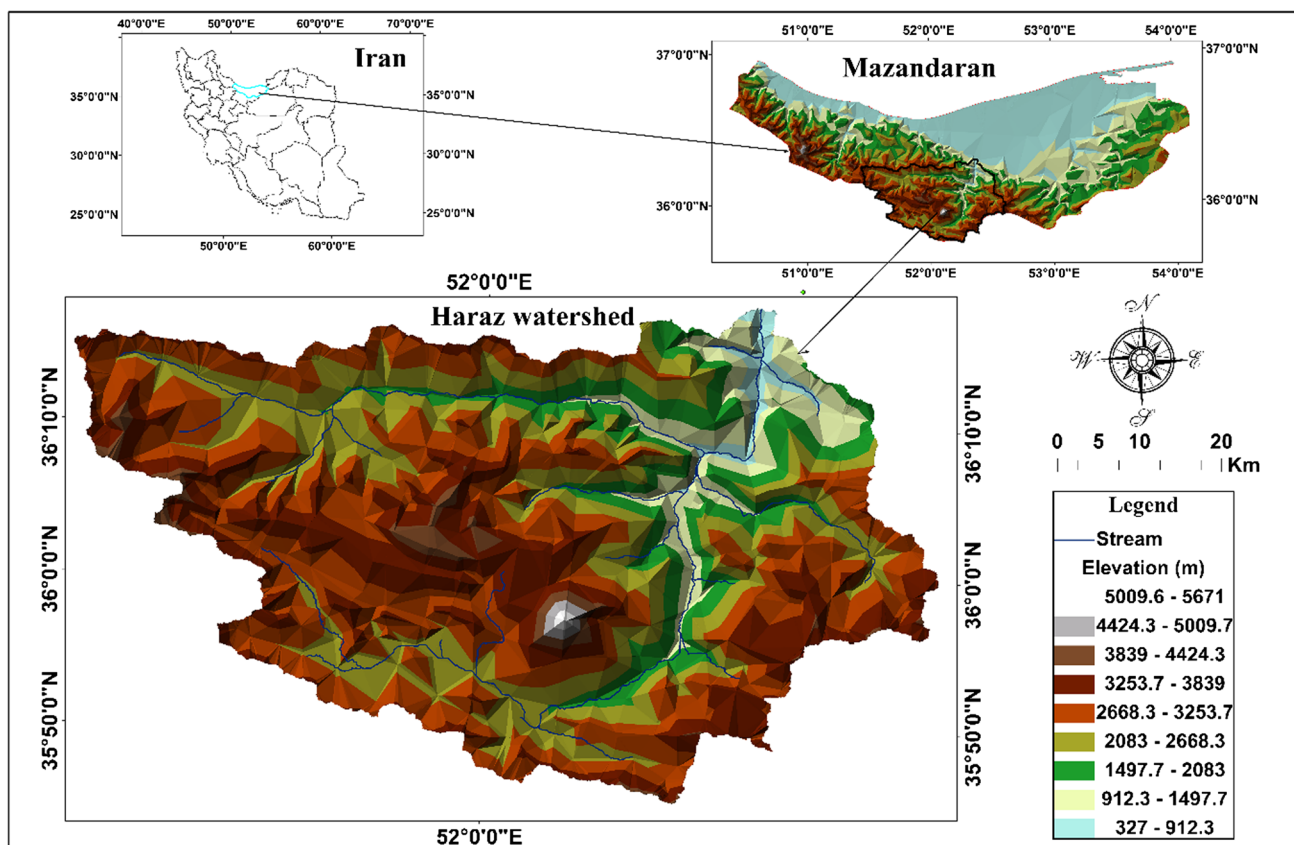


Fig. 1 Map of the study area

direct relationship with erodibility, and the shape sub-criteria such as circularity ratio and form factor have an inverse relationship with erodibility (Nooka Ratnam et al. 2005; Javed et al. 2009). The basin area, perimeter, stream order, basin length, stream length, elevation and streams number are calculated using ArcGIS10 software. The formulas used for the derivation of the morphometric sub-criteria of sub-watersheds are given in Table 1.

Topography

The topographic criteria was divided into three sub-criteria including LS-factor, elevation and aspect. The topography LS-factor showed length, slope gradient and the slope shape impact on the sediment yield (Pradhan et al. 2011). Estimation of the slope length is very time-consuming and cumbersome. For the method used in this study to obtain LS-factor, a program was written in Arc Macro Language (ALM) (Hichey 2000) and has been updated in 2004 with the C++ programming language. This program can be downloaded from the Web site: <http://www.iamg.org>. It used automatically with the DEM input to estimate the LS-factor (Van Remortel et al. 2004).

The elevation and aspect maps are provisioned the DEM with a pixel size of 30 m using ArcGIS software. Also in accordance with the objectives of the study, maps were divided using reclassify tools.

Soil

The soil is the eroded object, and soil erodibility represents rate of soil susceptibility to erosion, measured under standard plot conditions (Parysow et al. 2003). The soil erodibility factor (K) is related to organic matter content, permeability, soil texture and other factors (Wischmeier et al. 1971). In this study, the soil erodibility factor was determined using the Wischmeier and Smith equation (Eq. 1) (Wischmeier and Smith 1978).

$$100K = 2.1M^{1.14} \times 10^{-4} \times (12 - \%OM) + 3.25(S - 2) + 2.5(P - 3) \quad (1)$$

where K is the soil erodibility factor, M is the particle size parameter ($\% \text{ silt} + \% \text{ very fine sand} \times (100 - \% \text{ clay})$), OM is the organic matter content (%), S is soil structure, and P is the soil permeability class.

In this study, another sub-criterion of the soil was infiltration. There are the multiple methods to calculate the

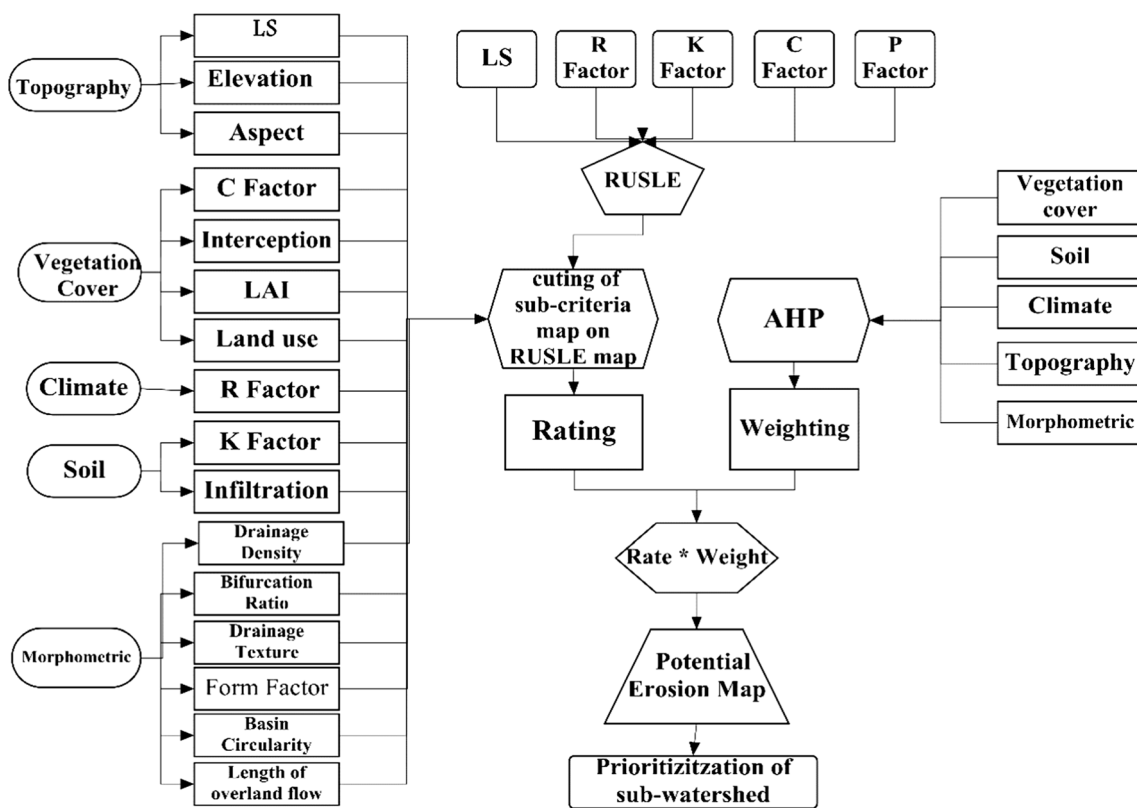


Fig. 2 Flowchart of general methods

Table 1 Formulae used for computation of morphometric sub-criteria

S. No.	Morphometric sub-criteria	Formulae*	Reference
1	Stream order	Hierarchical rank	Strahler (1964)
2	Stream length (Lu)	Length of the stream	Horton (1945)
3	Bifurcation ratio (Rb)	$Rb = N_u / N_{u+1}$	Schumm (1956)
4	Drainage density (D)	$D = Lu/A$	Horton (1932)
5	Drainage texture (Rt)	$Rt = Lu/P$	Horton (1945)
6	Form factor (Rf)	$Rf = A/Lb^2$	Horton (1932)
7	Circularity ratio (Rc)	$Rc = 4 * \pi * A/P^2$	Miller (1953)
8	Length of overland flow (Lg)	$Lg = 1/D * 2$	Horton (1945)

* N_1 No. of stream of one order, N_u No. of stream of final order; Lu = Total stream length of all orders; Nu = Total no. of streams of all orders, N_{u+1} Number of segments of the next higher order. A area of the basin (km^2), P perimeter (km), Lb basin length; π = 'Pi' value i.e., 3.14, D Drainage density

infiltration rate. The US Natural Resource Conservation Service (NRCS) had been classified soils into four hydrologic groups based on infiltration characteristic of the soils (Natural Resources Conservation Service Soil Survey Staff 1996). In this study, soil infiltration is defined using four hydrologic groups of soil. Guideline used by USDA soil survey to estimate soil infiltration into hydrologic groups is summarized in Table 2 (Arnold et al. 2012).

Finally, K-factor and infiltration data are fitted to the exponential model for experimental semivariograms. The K-factor and infiltration values at the observation points are

used for predicting the values of unknown points using the kriging interpolation method by the resulted model and parameters the semivariogram. The GS+9 software was used to perform semivariogram computation, and also the ArcGIS10 software was used for preparation of the spatial maps (Garcia-Mozo et al. 2006).

Climate

Rainfall erosivity has a direct relationship with soil erosion (Angulo-Martinez and Begueria 2009; Kaviani et al. 2011);

Table 2 Hydrologic Group rating infiltration (Arnold et al. 2012)

Hydrologic soil Group	A	B	C	D
Final constant infiltration rate (mm/h)	7.6–11.4	3.8–7.6	1.3–6.8	0–1.3

therefore, it was considered as a climate sub-criteria. In this study, the rainfall erosivity was calculated using an average annual rainfall data of 14 stations with a period of 42 years (1971–2013). Renard and Freimund (1994) calculated R-factor using Wischmeier’s research and monthly and annual rainfall data.

In this study, the annual rainfall erosivity is calculated using the Renard and Freimund (1994) method (Eqs. 2–4) (Relationship based on average monthly and annual rainfall data).

$$R = 0.7397F^{1.847}, \quad F < 5 \text{ mm} \quad (2)$$

$$R = 95.77 - 6.081F + 0.477F^2, \quad F > 55 \text{ mm} \quad (3)$$

$$F = \sum_{i=1}^{15} P_i^2 / \bar{P} \quad (4)$$

where F is the modified index value, P_i is average monthly precipitation, \bar{P} is average annual precipitation, and R is rainfall erosivity factor to unit $\text{MJ mm ha}^{-1} \text{ h}^{-1} \text{ year}^{-1}$. Then, characteristics of variogram model were given to ArcGIS software, and R-factor map was drowned using the kriging method (Kavian et al. 2011).

Vegetation cover

In this study, four sub-criteria of vegetation cover including C-factor, leaf area index (LAI), interception and land use were identified. Different methods have been developed to estimate C-factor to evaluate soil loss using Normalized Different Vegetation Index (NDVI) by various researchers (De Jong 1994; Lin et al. 2002; De Jeng 1999; Wang et al. 2002). NDVI is derived from the near infrared band and red band of the remote sensing data (Eq. 5) (Zhang et al. 2010).

$$NDVI = (\rho_{NIR} - \rho_{Red}) / (\rho_{NIR} + \rho_{Red}) \quad (5)$$

where ρ_{Red} is red band and ρ_{NIR} is near infrared.

Final C-factor of watershed is prepared using Eq. 6.

$$C \text{ Factor} = 0.407 - 0.5953 \times NDVI \quad (6)$$

Since the amount of LAI is influenced from the remote sensing signals at different wavelengths, regional and global LAI maps can be extracted from remote sensing multispectral images (Lim et al. 2005). The LAI of the study area was calculated using Eq. (7).

$$LAI = -\ln(0.69 - SAVI_{ID}/0.59)/0.91 \quad (7)$$

The SAVI is an index that soil impacts reduced from NDVI on surface earth, so that impact of soil moisture is reduced in the index. The SAVI is calculated using Eq. (8).

$$SAVI = (1 + L)(\rho_{NIR} - \rho_{Red}) / (L + \rho_{NIR} - \rho_{Red}) \quad (8)$$

Branch and leaf plant prevent from direct reach of rainfall to the ground. That part of the rain is taken by vegetation that is called rainfall interception (Chow et al. 1988). The rainfall interception is calculated using Eq. (9).

$$ScMSX = 0.935 + 0.498LAI - 0.00575LAI^2 \quad (9)$$

The land-use map was carried out using the satellite images of 2013 that were downloaded from the USGS site with preprocessing and processing and final post-processing. Satellite images were divided into seven classes of forest, rangeland, bare land, garden, irrigated land, residential and waterbody. According to the selected bands, the land-use map was obtained using maximum likelihood algorithm and evaluated by the ground truth map and field operations and topographic maps. Since constitution of error matrix was accomplished by assessment of classification result accuracy based on criteria, overall accuracy, kappa coefficient, producing accuracy and user accuracy (Kelarestaghi and Jafarian Jeloudar 2011).

Estimation of soil erosion risk by RUSLE

The Revised Universal Soil Loss Equation (RUSLE) has used to estimate soil erosion risk in study area. The average annual soil loss (A) in tons per hectare per year is calculated using RUSLE by the following equation Eq. (10) (Renard et al. 1997):

$$A = R \times K \times LS \times C \times P \quad (10)$$

where w is the average annual soil loss ($\text{ton ha}^{-1} \text{ year}^{-1}$); R rainfall erosivity factor [$\text{MJ mm} \cdot (\text{ha}^{-1} \text{ h}^{-1} \text{ year}^{-1})$]; K is the soil erodibility factor [$\text{ton ha}^{-1} \text{ h MJ}^{-1} \text{ ha}^{-1} \text{ mm}^{-1}$]; LS is the slope length and slope gradient factor (dimensionless); C is the cover management practice factor (dimensionless); and P is the conservation support or erosion control practices factor (dimensionless).

Sub-criteria rating

In this research, analysis of erosion-prone in order to implement sub-criteria rating is used from frequency ratio method. Frequency ratio method (w) is examined based on the correlation of overlay between erosion hazard map (which in this study was considered RUSLE map) and features maps of various factors. In this study, frequency ratio (w) is obtained using the following formula for each

class of sub-criteria Eq. (11) (van Westen 1997; Kelarestaghi and Jafarian Jeloudar 2011).

$$W = \ln(Densclass/Densmap) = \ln[(Npix(Si)/Npix(Ni)) / (SNpix(Si)/SNpix(Ni))] \quad (11)$$

where W is frequency ratio, $Npix(Si)$ is the number of pixels or area that contain erosion hazard in a certain parameter class, $Npix(Ni)$ is the total number of pixels or area in a certain parameter class, $SNpix(Si)$ is the total number of pixels or area that contain erosion hazard in a certain parameter class, and $SNpix(Ni)$ is the total number of pixels or area in a watershed area.

Criteria weighting

The analytical hierarchy process (AHP) technique has been applied for soil erosion hazard assessment and analysis, especially to define the factors that influenced on the soil erosion and to derive their weights (Alexakis et al. 2013; Kachouri et al. 2014). Weights of each criterion are obtained based on a pairwise comparison matrix, and hence, each criterion is assigned a weight based on its significance relative to each of the other criterion (Kachouri et al. 2014). In the criteria, weighting is used from comparison between the criteria by oral judgments of experts.

Potential erosion mapping

Finally, soil erosion-prone of the study area is calculated by multiplying the weight of each criterion in sub-criteria class ratio and sum of these numbers Eq. (12).

$$M = a_1x_1 + a_2x_2 + a_3x_3 + a_4x_4 + a_5x_5 \quad (12)$$

where a_1 – a_5 is the weight coefficients and x_1 – x_5 is the sub-criteria class ratio. The map of potential erosion was obtained by combining data of 16 sub-criteria maps. The map of potential erosion was classified in three levels of hazard of low, moderate and high.

Prioritization of sub-watershed

The amounts of weight average were used to prioritize sub-watersheds and identify erosion susceptible region. The sub-watershed with the highest weight value is most susceptible to erosion and needs highest priority for soil conservation measures. Based on average weight value, sub-watersheds were categorized into three priority groups.

Results and discussion

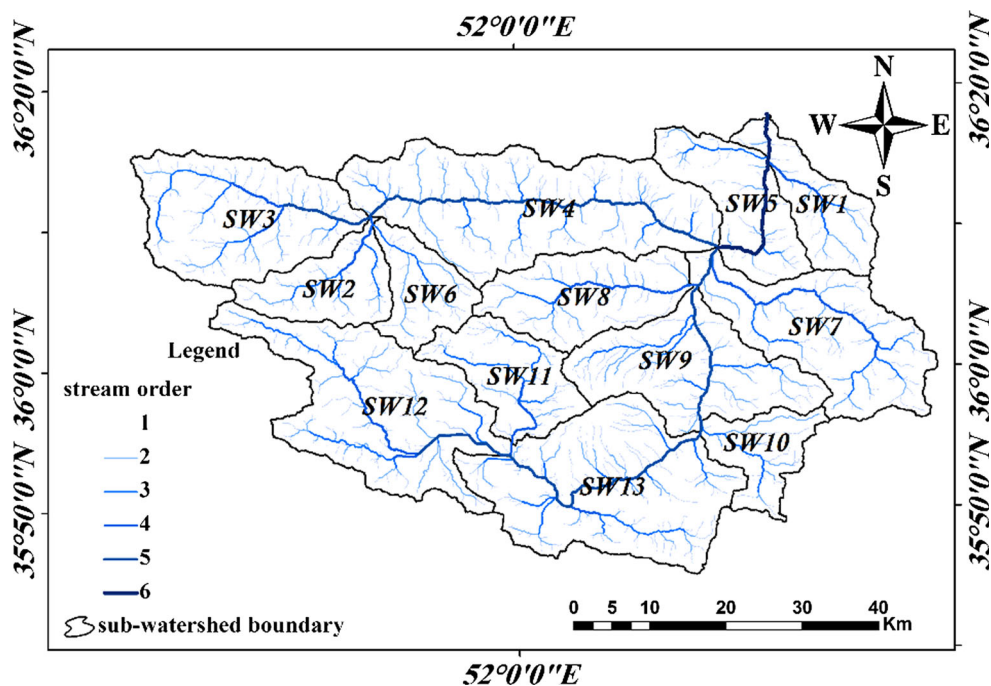
Morphometric

The map of stream order was provisioned using of Strahler method (Fig. 3) that is a usual method for order of streams. In morphometric studies, the measurement of various drainage network indices is used for assessing the effect of stream characteristics on the land surface processes occurring over a landscape. Morphometric factors was calculated the using various drainage characteristics such as basin area, perimeter, basin length, stream length and stream order (Kumar et al. 2000; Altaf et al. 2014). The maps of classed morphometric parameters have showed in Fig. 4. The results showed that by increasing the liner parameters value such as bifurcation ratio, length of overland flow, drainage density and drainage texture, erodibility potential has increased, while by increasing the shape parameter such as basin shape and circulatory ratio, erodibility potential has decreased. The shape of the watershed affects the stream flow hydrography, peak flows (Gajbhiye et al. 2014) and soil infiltration. Soil infiltration is less in the basins with lower value of shape parameter; therefore, soil erosion is higher. Also, Ahmad Dar et al. (2013) concluded that basin soil erosion will increase by increasing the drainage density. Also, Altaf et al. (2014), Nooka Ratnam et al. (2005), Javed et al. (2009), Avinash et al. (2011) and Gajbhiye et al. (2014) founded that the linear parameters have a direct relationship with erodibility, and the shape parameters have an inverse relationship with erodibility.

Topography

The LS-factor map was calculated using DEM of watershed that indicant slope gradient and length in watershed area. The LS-factor value was in the range of 0–252 with a mean value of 12.5 and a standard deviation of 13.26. The LS-factor value mentioned to change very violent topography in the Haraz watershed (Fig. 6c). The LS-factor classes had the value of 0–12, 12–32 and more than 32, which indicates that their spatial coverage in the watershed was 62.72, 29.7 and 7.67 %, respectively. Basin slope has direct relationship and fair complex with water infiltration, surface runoff and soil moisture that effective on basin soil erosion and sediment yield. By increasing the amount of LS, soil erosion increased in the study area that correspond with results of Renard et al (1997) and Wischmeier and Smith (1978). Increasing of the slope gradient and length increased velocity of water on the ground surface and finally, giving rise to greater soil erosion rates (Haan et al. 1994).

Fig. 3 Stream order map



The aspect has an indirect effect on the soil erosion (Morgan 2005). The aspect map was calculated using DEM of watershed (Fig. 6a). The north aspects of study region with area of 30.94 % and maximum weight value had showed the greatest impact on the erosion basin. The aspects of south with area of (28.30 %), east (21.01 %), west (19.47 %) and flat (0.26 %) had showed the most to least impact, respectively, on the erosion hazard. Increasing erosion is due to more precipitation and rainfall erosivity and also increasing soil moisture causes mass movement in the north aspect that are the most important factors in the soil erosion.

The elevation map of the study area was prepared by the ArcGIS software and was divided into three classes (Fig. 6b). The elevation of 3000–5610 m showed the most impact in the Haraz watershed erosion. The elevation of study area increases from the northeastern to the west of basin. Soil erosion has increased with increasing elevation in the study area. There is near relationship between topography characters and soil erosion; therefore, the implementation of conservation practices is essential in the high elevation region, especially elevation of 4000–5610 m with frequency of erosion hazard area of 44.75 %. The slope and amount of rainfall erosivity have increased with increasing the elevation while decreased vegetation dispersion that directly affected on the soil erosion.

Climate

Climate is one of the most important parameters that effected directly and indirectly on the soil erosion (Bouaziz

et al. 2011). Rainfall erosivity (R) value was calculated using Freimund method by the annual and the monthly rainfall data. Figure 5c and Table 3 shows the variogram model and parameters of R-factor, respectively. The average annual R-factor value varies from 170 to 541 MJ mm ha⁻¹ h⁻¹ year⁻¹ with a mean value of 351.12 MJ mm ha⁻¹ h⁻¹ year⁻¹ in the watershed. Figure 6d shows the R-factor map of the study area. According to the map, amounts of rainfall erosivity decrease from the south to the north of the basin that showed rainfall reduction and non-uniform spatial distribution in the basin (Kouli et al. 2009). The literature review indicates that R-factor has correlated highly with soil erosion in the many parts of the world (Wischmeier and Smith 1978; Renard and Freimund 1994; Ferro et al. 1991). The rainfall erosivity factor (R) represents the effect of rainfall intensity on soil erosion and also the rain drop created soil splash that transported soil particles on the ground surface.

Soil

Figure 5b and Table 4 show the variogram model and parameters of K-factor, respectively. The maximum spatial correlation was calculated 30,400 m (Table 4). K-factor map produced in the spatial analysis tool of the ArcGIS10 by means of variogram models and parameters and obtained a high quality map (Fig. 6f). The K-factor value varied between 0.16 to 0.34 t ha h MJ⁻¹ and average value of 0.24 t ha h MJ⁻¹ in the basin. The higher values were showed in the west part of the catchment and lower values were showed in the east part of the catchment. The higher

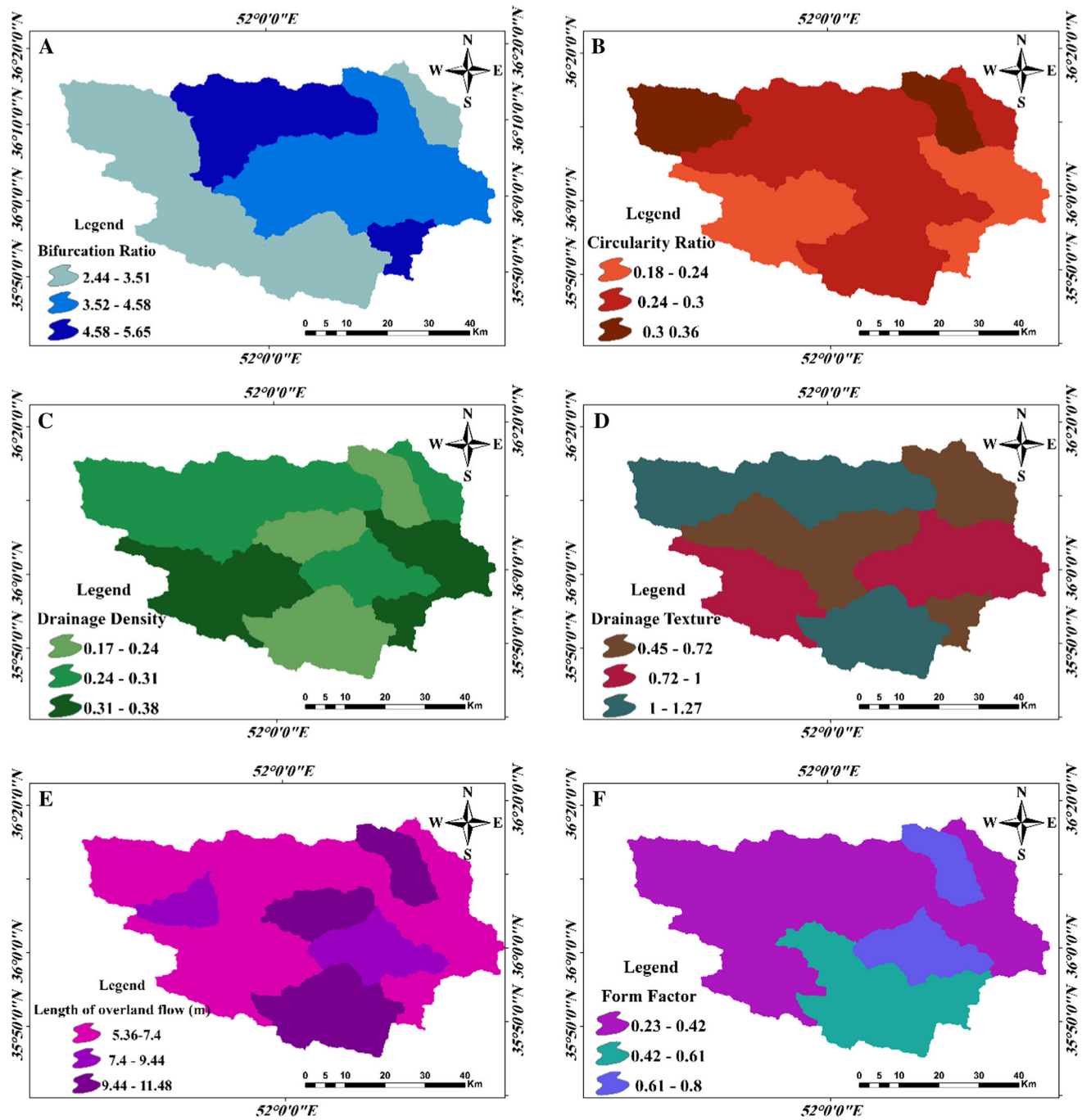


Fig. 4 Morphometric parameters classification maps: **a** Bifurcation ratio, **b** Circularity ratio, **c** Drainage density, **d** Drainage texture, **e** Length of overland flow, **f** Form factor

values of k-factor indicate high amount of silt and very fine sand particle that causes increased soil erosion in the catchment (Kamaludin et al. 2013).

The amount of runoff and consequently soil erosion will reduce with increasing of the soil infiltration rate, because infiltration prevented from creating runoff from rainfall and soil loss. Therefore, increasing of the soil infiltration is one of the ways to prevent soil erosion (Morgan 2005).

Figure 5a and Table 5 shows the variogram model and parameters of infiltration, respectively. The maximum spatial correlation was calculated 11,140 m (Table 5). The soil infiltration map produced using parameters and variogram model by the spatial analysis tool of ArcGIS10 (Fig. 6l). The soil infiltration value varies from 0.65 to 9.49 mm/h with a mean value of 5.16 mm/h in the catchment. Considering the map, the northern parts of the basin

Fig. 5 Variogram of sub-criteria: **a** variogram of infiltration, **b** variogram of K-factor, **c** variogram of R-factor

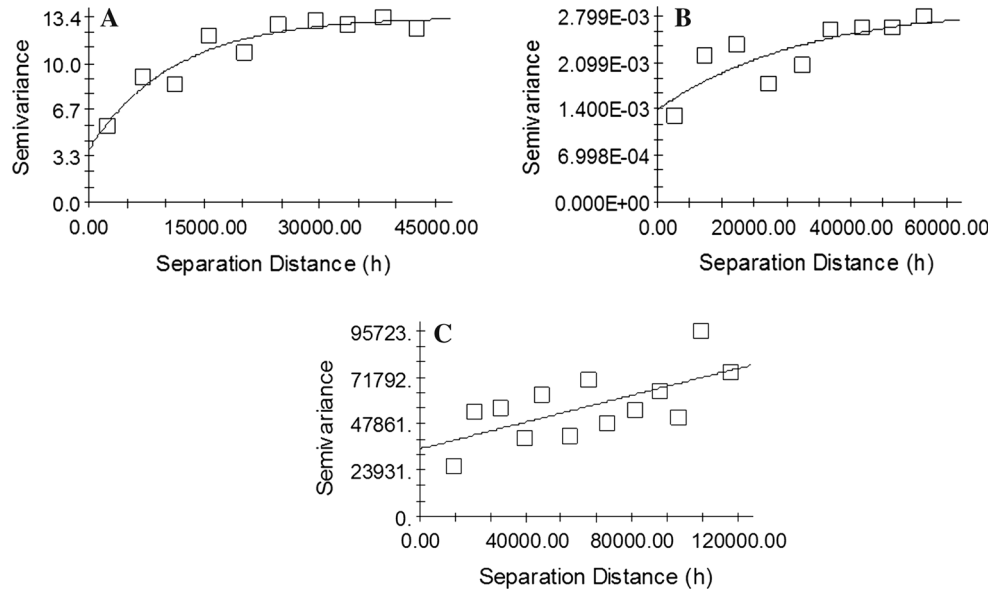


Table 3 Parameters of the fitted variogram for R-factor

Variable	Model	C0	C0 / (C0 + C)	C0 + C	A0	RSS	R2
R-factor	Line	97,000	0.880	805,000	131,300	1.325E+11	0.683

have the highest infiltration rate, and the western parts of the basin have the lowest infiltration rate.

Vegetation cover

C-factor map was prepared using NDVI map (Fig. 6j). The value for C-factor ranges from 0.08 to 0.53 with a mean value of 0.34. The highest value (low soil protection) was in the central, north and west part, while the northeast part of the basin had the smallest value because the forest cover. Soil erosion has increased with increasing C-factor that is consistent with results of Kouli et al. (2009), Gitas et al. (2009) and Sun et al. (2014).

Figure 6g shows the land-use map of the study area. The range coverage is first dominant factor with 75.85 % in the study area. The coverage percentages of forest, bare land, irrigated land, garden and residential are 6.08, 8.95, 3.62, 3.22 and 2.16 %, respectively. The bare land has highest amount of soil erosion in between different land use. The vegetation parameters are a factor affecting on soil erosion hazard in different area (Bouaziz et al. 2011).

The maps of the LAI and the rainfall interception were prepared using satellite image (Fig. 6h, l). The value of LAI ranges from 0 to 0.96. The value of rainfall interception ranges from 0.47 to 1.41 with a mean value of 0.91. The highest value of the rainfall interception and the LAI was in the northeast part because forest cover. The lowest value of the rainfall interception and the LAI was in the north and center part of basin that have low vegetation cover and bare land. The

rainfall interception and the LAI are prevented from direct clash of raindrop and increased infiltration and consequently reduced rainfall erosivity. Regions with highest value of rainfall interception and the LAI have lowest soil loss.

RUSLE erosion risk

The annual soil loss (A) was calculated using of the RUSLE model in the ArcGIS10 environment, in order to calculate the soil loss for each individual grid cell (Farhan and Nawaiseh 2015). The annual soil loss values range between 0 and 5621 ton ha⁻¹ year⁻¹ (Fig. 7).

Sub-criteria rating

The low rate represents a low hazard of erosion risk, while high rate represents a high hazard of erosion. Table 6 shows the rate of sub-criteria. The classes of 32>, 12–32 in the LS-factor, 4.58–5.65 in the bifurcation ratio and 0.1–0.9 in the LAI factor had the highest rate of 2.3, 1.89, 1.65, 1.61, respectively. Also classes of water body in the land use, 0–0.1 in the LAI factor, 0–12 in the LS-factor and 0.08–0.25 in the C-factor had the smallest rate of 0.12, 0.28, 0.38 and 0.51, respectively.

Criteria weighting

AHP techniques were used to assessment weights of the criteria. In this study, the aim of was to determine the

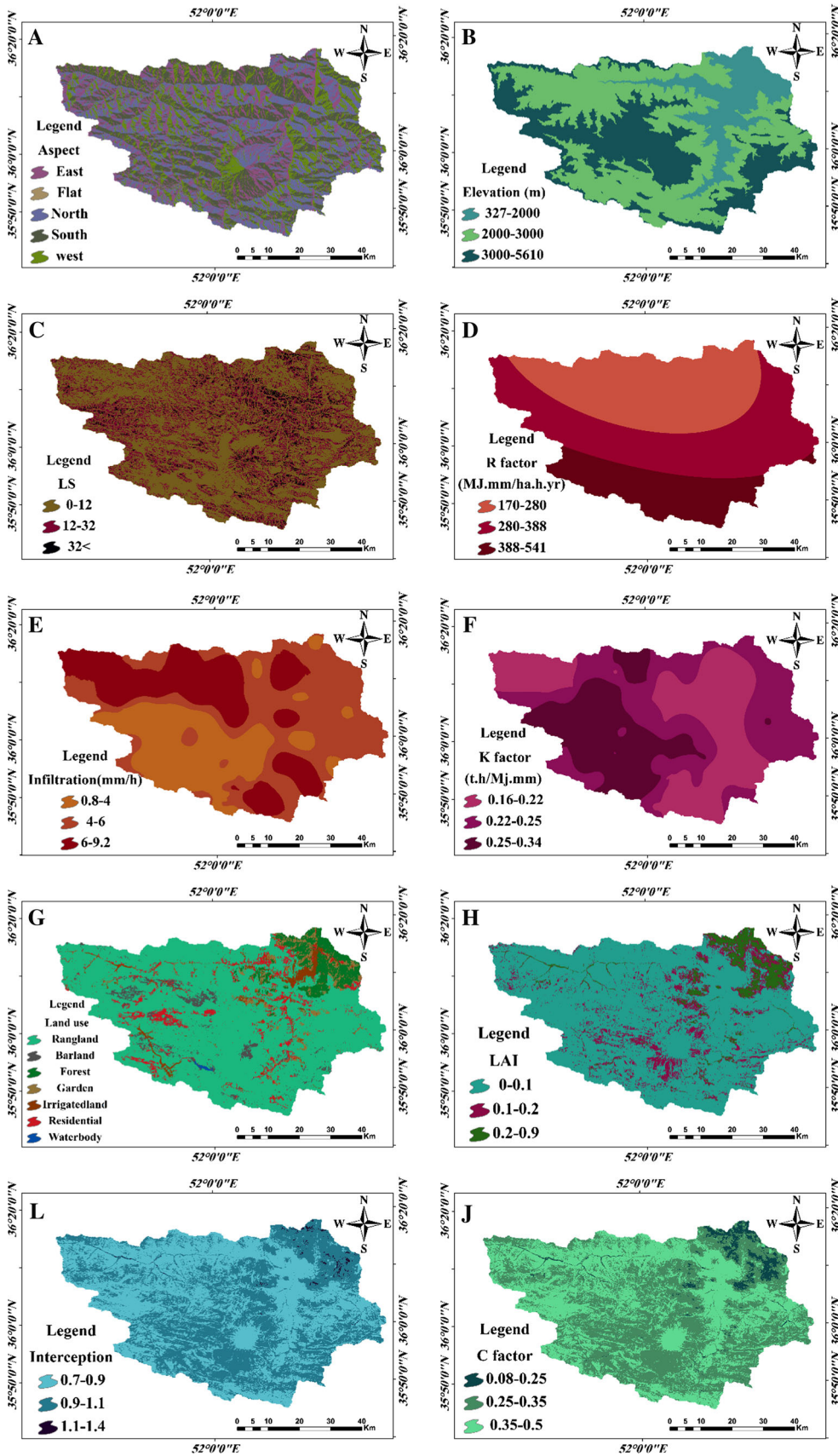


Fig. 6 Maps of sub-criteria: **a** Aspect map, **b** Elevation map, **c** LS map, **d** R-factor map, **e** Soil infiltration map, **f** K-factor map, **g** land-use map, **h** LAI map, **i** Rainfall interception map, **j** C-factor map

weight of criteria which were used 30 questionnaires by experts. The results of the criteria weights are shown in Fig. 8. The quality of the comparison is described by the consistency ratio that ranges from 0 to 1 (Kachouri et al. 2014). In the current study, the consistency ratio of the matrix of the five influence criteria is 0.06. The topography has the most weight, and the soil factor has the lowest weight. The topography and the soil have the highest and the lowest effective, respectively, on the erosion hazard in the Haraz watershed.

Map of potential erosion

The map of potential erosion was classified in three levels of hazard of low, moderate and high. Lands of the study area have largely moderate (37.86 %) potential to erosion.

The area of low and high erosion hazard corresponds to 30.37 and 31.76 %, respectively. The spatial distribution of soil erosion hazard (Fig. 9) shows that the hazard condition is high in the west part of Haraz watershed due to impact of the poor vegetation and the factors of topographies and soils. This result with results of Benkobi et al. (1994) and Biesemans et al. (2000) had considered that expressed vegetation, slope length and slope gradient factor have more sensitive in soil erosion and sediment yield. Also, sun et al. (2014) had founded that land use and vegetation are an important factor and affecting in the soil erosion. Low soil erosion zone is shown in the east north of Haraz watershed, and this could be explained due to the area mostly covered by dense vegetation of forest (Arar and Chenchouni 2012). Moreover, these vegetation cover have higher soil preservation value and the low of soil erosion susceptibility (Arar and Chenchouni 2014). Indeed, the presence of friable soil with the absence of the vegetation cover on the ground surface allows the transport of soil particles by runoff (FAO 1989; Bachaoui et al. 2007).

Table 4 Parameters of the fitted variogram for K-factor

Variable	Model	C0	C0/(C0 + C)	C0 + C	A0	RSS	R2
K-factor	Exponential	0.001	0.529	0.003	30,400	6.414E-07	0.657

Table 5 Parameters of the fitted variogram for infiltration

Variable	Model	C0	C0/(C0 + C)	C0 + C	A0	RSS	R2
Infiltration	Exponential	3.79000	0.529	13.33000	11,140	5.07	0.915

Fig. 7 Soil erosion risk map (RUSLE)

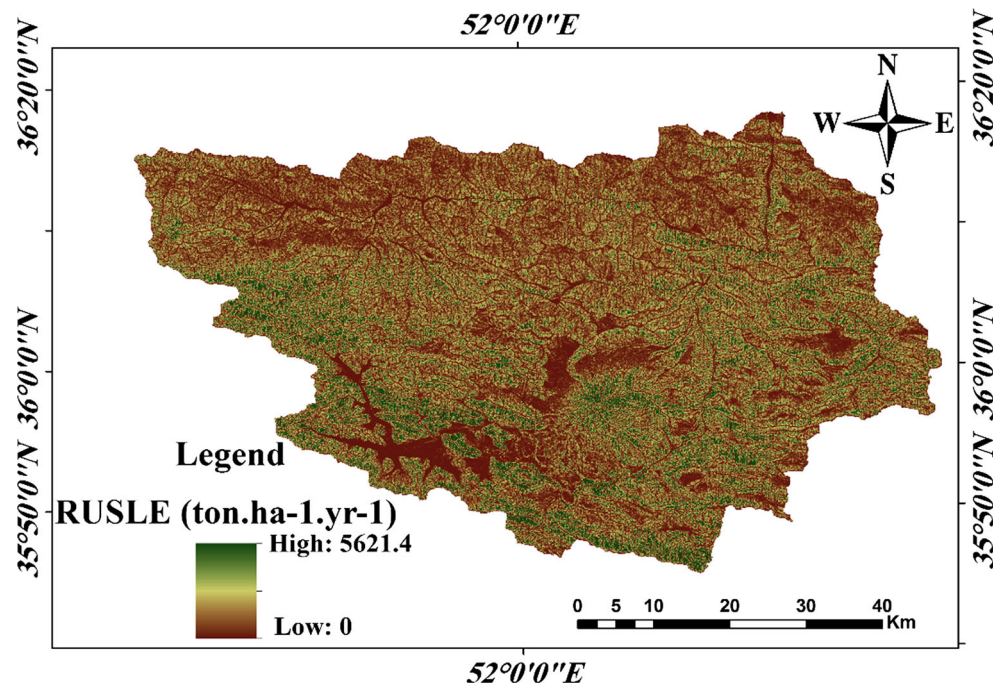


Table 6 Values of rate and weight of sub-criteria

Criteria	Sub-criteria	Class	Total area (km ²)	Erosion area (km ²)	Rate	Weight	Final weight
Topography	Aspect	South	1136.03	455.44	1.01		0.34
		North	1242.16	568.71	1.15		0.39
		East	843.44	279.7	0.83		0.28
		flat	10.5	2.96	0.71		0.24
		West	781.8	285.55	0.92		0.31
	Elevation	327–2000	644.2	248.14	0.97	0.342	0.33
		2000–3000	1993.85	719.03	0.91		0.31
		3000–5610	1376.06	625.22	1.14		0.39
	LS	0–12	2517.74	379.06	0.38		0.13
12_32		1188.28	932.6	1.98		0.67	
32<		307.96	280.692	2.3		0.78	
Soil	K-factor	0.16–0.22	1392.31	541.28	0.98		0.1
		0.22–0.25	1556.1	580.1	0.94		0.1
		0.25–0.34	1065.75	471.05	1.11		0.12
	Soil infiltration	0.8–4	1133.81	497.25	1.1	0.111	0.12
		4–6	1666.9	684	1.03		0.11
		6–9.2	1213.45	411.17	0.85		0.09
Climate	R-factor	170–280	1548.58	498.56	0.81		0.19
		280–388	1652.48	736.97	1.12	0.24	0.27
		388–541	812.99	356.89	1.1		0.26
Vegetation	C-factor	0.08–0.25	142.7	28.83	0.51		0.08
		0.25–0.35	1950.01	711.25	0.92		0.14
		0.35–0.5	1921.45	852.36	1.12		0.17
	Rainfall interception	0.7–0.9	2169.87	951.39	1.1		0.17
		0.9–1.1	1822.38	638.18	0.88		0.13
		1.1–1.4	21.91	2.88	0.33		0.05
	Land use	Bare land	128.86	62.68	1.22		0.19
		Irrigated land	123.32	33.63	0.68	0.158	0.1
		Garden	124.43	38.16	0.77		0.12
		Residential	239.4	94.89	1		0.15
		Forest	220.9	68.4	0.78		0.12
		Range	3173.18	1294.36	1.03		0.16
Water body		4.72	0.23	0.12		0.02	
LAI	0–0.1	3289.2	1382.61	1.06		0.16	
	0.1–0.2	482.54	54.74	0.28		0.045	
	0.2–0.9	242.43	155.1	1.61		0.25	
Morphometric	Bifurcation ratio (Rb)	2.44–3.51	1744	738	1.06		0.15
		4.58–5.65	859	563	1.65		0.24
		3.52–4.85	1387	289	0.52		0.07
	Drainage density (D)	0.24–0.31	1786.1	633.82	0.89		0.13
		0.17–0.24	1007.68	419.23	1.05		0.15
		0.31–0.38	1195.45	536.85	1.13		0.16
	Length of overland flow (Lg)	5.36–7.4	2471.45	925.77	0.94	0.149	0.14
		7.4–9.44	510.09	244.9	1.21		0.18
		9.44–11.48	1007.68	419.23	1.05		0.15
	Circularity ratio (Rc)	0.24–0.3	2192.21	864.21	0.99		0.14
		0.3 0.36	601.57	188.84	0.79		0.11
		0.18–0.24	1195.45	536.85	1.13		0.16

Table 6 continued

Criteria	Sub-criteria	Class	Total area (km ²)	Erosion area (km ²)	Rate	Weight	Final weight
0.72–1	Form factor (Rf)	0.23–0.42	2565.72	984.5	0.96	0.17	0.14
		0.61–0.8	558.41	227.74	1.02		0.15
		0.42–0.61	865.1	377.66	1.1		0.16
	Drainage texture (Rt)	0.45–0.72	1266.41	489.32	0.97		0.14
		1–1.27	1513.01	535.26	0.89		0.13
		1209.81	565.32	1.18			

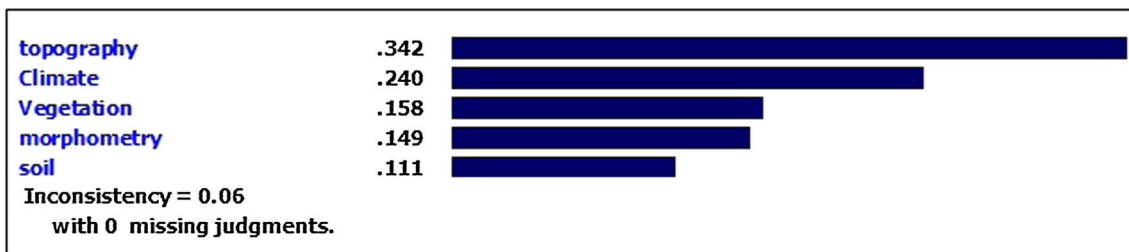
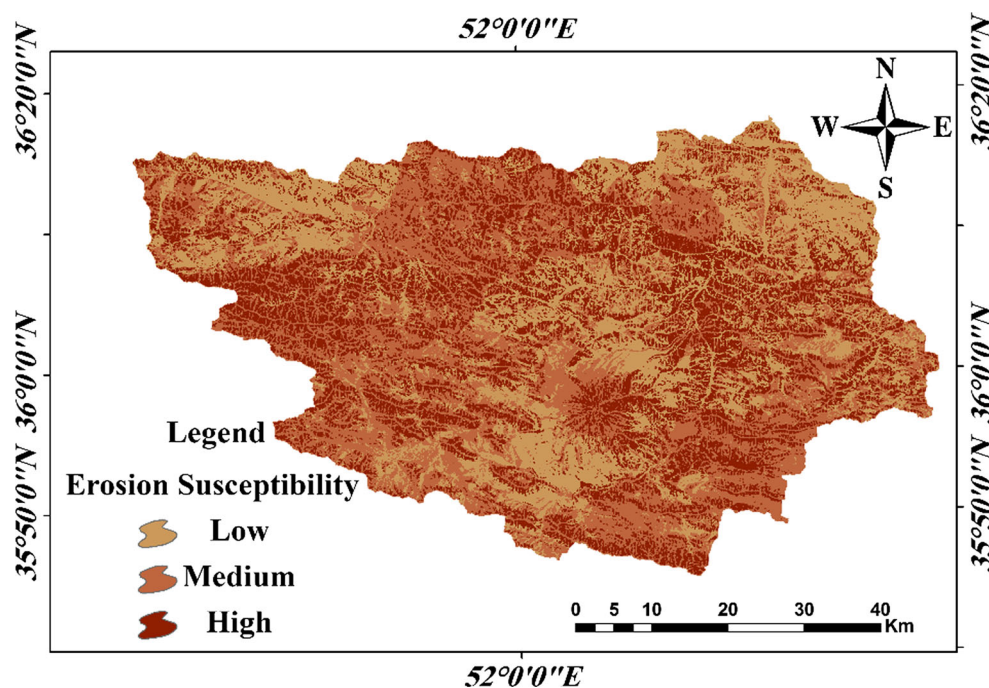


Fig. 8 Criteria weight

Fig. 9 Map of erosion susceptibility priority in the study area



Prioritization of sub-watershed

Amounts of 13 sub-watershed weight value (maximum, minimum, average and standard deviation) were calculated for prioritization of sub-watershed (Table 7). Based on average weight value, sub-watersheds were categorized into high priority (3.1–3.2), medium priority (3–3.1) and low priority (2.89–3). Figure 10 shows priority of sub-watershed for planning soil and water conservation.

High priority

Out of the total 13 sub-watersheds, two sub-watersheds of SW10 and SW2 came under the high priority and cover 7.47 % of study area. These sub-watersheds have highest value of slopes, elevation and K-factor as compared to other sub-watersheds. Also, these sub-watersheds have low soil infiltration and limited vegetation cover (low LAI, rainfall interception and C-factor), the bare land surfaces

Table 7 Weight values and prioritization of the Haraz sub-watershed

Sub-basin	Min	Max	Average	Standard deviation	Rank	Prioritization
SW1	2.41	3.6	2.89	0.25	13	Low
SW2	2.55	3.77	3.18	0.29	2	High
SW3	2.49	3.68	2.99	0.26	10	Low
SW4	2.5	3.73	3.1	0.27	5	Medium
SW5	2.37	3.49	2.9	0.28	12	Low
SW6	2.55	3.75	3.14	0.27	3	Medium
SW7	2.42	3.63	3.05	0.26	8	Medium
SW8	2.4	3.61	2.98	0.28	11	Low
SW9	2.48	3.67	3.06	0.28	7	Medium
SW10	2.73	3.89	3.26	0.27	1	High
SW11	2.56	3.66	3	0.24	9	Low
SW12	2.62	3.75	3.12	0.27	4	Medium
SW13	2.56	3.77	3.07	0.28	6	Medium

and poor rangeland cover. Hence, these sub-watersheds have higher erosivity, thus needing immediate attention for implementation of soil and water conservation practices.

Medium priority

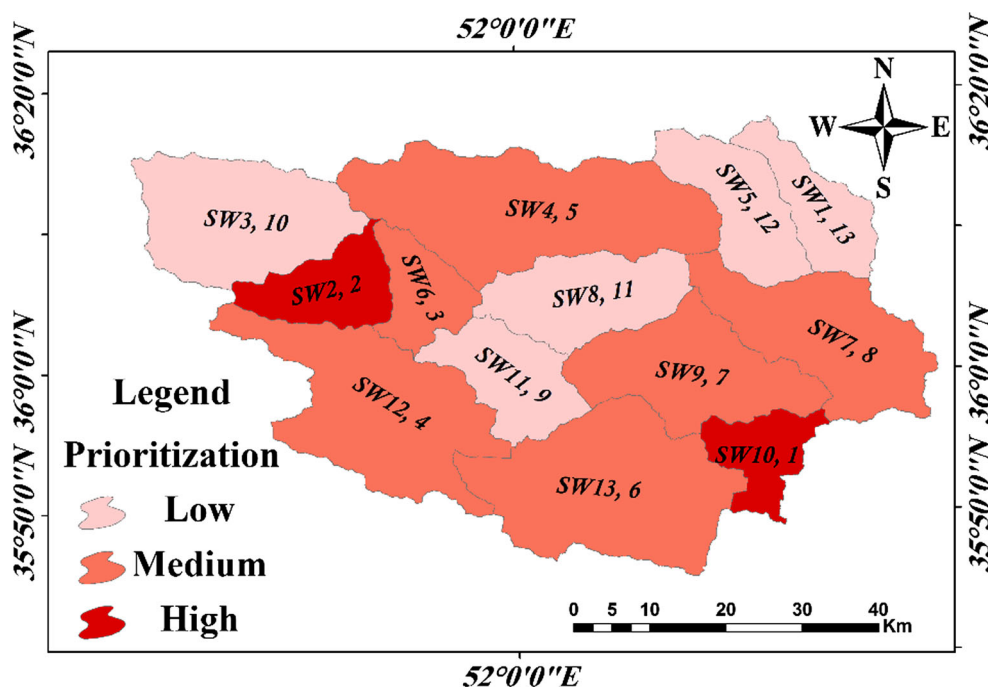
Six sub-watersheds of SW4, SW6, SW12, SW13, SW9 and SW7 fall under medium priority and cover 62 % of the study area. These sub-watersheds have medium value of LS-factor, K-factor, soil infiltration, rainfall interception, LAI and R-factor when compared to other sub-watersheds. Therefore, these six sub-watersheds do not suffer from any significant hazards and need no immediate

attention for implementation of soil and water conservation practices.

Low priority

Five sub-watersheds of SW1, SW5, SW8, SW11 and SW3 have been placed under low priority that covering an area of 30.53 % of the Haraz watershed area. These have lowest value of LS-factor, K-factor and elevation. Two sub-watersheds (SW1 and SW5) in the northeast part (watershed output) have good vegetation cover (forest). However, these sub-watersheds do not need immediate soil and water conservation, which is considered necessary.

Fig. 10 Sub-watershed prioritization map



Conclusions

Investigation on sub-watersheds for planning soil and water conservation is very important and vital issue aspect of watershed management. For this study, sub-criteria was rated by soil loss predictions RUSLE model and derived from frequency ratio method, and original criteria was weighted by AHP approach integrated with GIS and RS. The value of soil erosion hazard was calculated from 2.37 to 3.89 in the watershed area. According to the estimated amount of soil erosion, soil erosion hazard is relatively medium and in some areas is critical in the Haraz watershed. GIS and RS are fundamental tools to assess and identify soil erosion susceptibility region. Also, Kachouri et al. (2014) indicated that assessing spatial distribution of soil erosion hazard is possible by using three tools of remote sensing data, GIS and AHP method.

The factors that contribute to soil erosion potential in this watershed were analyzed. Evaluation of different sub-criteria in this study showed that increasing the amount of LS in the study area increased soil erosion that is consistent with results of Renard et al. (1997) and Wischmeier and Smith (1978). Vegetation, slope, soil texture and land use are critical factors in the soil erosion assessment (Le Bissonnais et al. 2001; Sahin and Kurum 2002; Kheir et al. 2006). The effective sub-criteria from high to low included LS, C-factor, elevation, aspect, R-factor, bifurcation ratio, length of overland flow, LAI, form factor, drainage density, drainage texture, basin circularity, land use, rainfall interception, K-factor and soil infiltration, respectively. Therefore, these factors should adopt for soil and water conservation in the catchment.

Out of 13 sub-watershed, SW10 and SW2 fall in high priority, SW4, SW6, SW7, SW9, SW13 and SW12 fall in medium priority, whereas SW1, SW5, SW8, SW11 and SW3 fall in low priority category in order to implementation of soil and water conservation practice. The susceptible sub-watersheds to soil erosion should be identified and implemented in the future projects based on protection priority. With regard to the problem of soil erosion, watershed comprehensive studies and practice of soil and water conservation is essential particularly in the sub-watersheds have critical conditions. The method presented in this study has been identified very good spatial distribution for soil erosion hazard mapping. This shows the good potential of this method in other areas in order to prioritize of sub-watersheds for soil and water conservation practice.

References

Abdul Rahamana S, Abdul Ajeezb S, Aruchamy S, Jegankumar R (2015) Prioritization of sub watershed based on morphometric characteristics using fuzzy analytical hierarchy process and

- geographical information system—a study of kallar watershed, Tamil Nadu. (Aquatic Procedia) International conference on water resources, coastal and ocean engineering (ICWRCOE 2015) vol 4, pp 1322–1330
- Ahmad Dar I, Prabu P, Ahmad Dar M (2013) Erosion modeling in hard rock terrain using morphometry: a case study from Tamilnadu, India. *Environ Qual Manag* 23(2):47–60
- Alexakis D, Hadjimitsis D, Agapiou A (2013) Integrated use of remote sensing, GIS and precipitation data for the assessment of soil erosion rate in the catchment area of “Yialias” in Cyprus. *Atmos Res* 131:108–124
- Altaf S, Meraj G, Romshoo S (2014) Morphometry and land cover based multi-criteria analysis for assessing the soil erosion susceptibility of the western Himalayan watershed. *Environ Monit Assess* 186(12):8391–8412
- Angulo-Martinez M, Begueria S (2009) Estimating rainfall erosivity from daily precipitation records: a comparison among methods using data from the Ebro Basin (NE Spain). *J Hydrol* 379:111–121
- Arar A, Chenchouni H (2012) How could geomatics promote our knowledge for environmental management in Eastern Algeria? *J Environ Sci Technol* 5(5):291–305
- Arar A, Chenchouni H (2014) A “simple” geomatics-based approach for assessing water erosion hazard at montane areas. *Arab J Geosci* 7(1):1–12
- Arnold J, Kinary J, Srinivasan R, Williams J, Haney E, Neitsch S (2012) Soil & water Assessment tool, Input/Output Documentation Version 2012. Texas water resources institute
- Avinash K, Jayappa K, Deepika B (2011) Prioritization of sub-basins based on geomorphology and morphometric analysis using remote sensing and geographic information system (GIS) techniques. *Geocarto Int* 26(7):569–592
- Bachaoui B, Bachaoui E, El Harti A, Bannari A, El Ghmari A (2007) Cartographie des zones à risque d'érosion hydrique: exemple du haut Atlas marocain. *Teledetection*. 7:393–404
- Benkobi L, Trlica M, Smith J (1994) Evaluation of a refined surface cover subfactor for use in RUSLE. *J Range Manage* 47:74–78
- Biesemans J, Meirvenne M, Gabriels D (2000) Extending the RUSLE with the Monte Carlo error propagation technique to predict long-term average off-site sediment accumulation. *J Soil Water Conserv* 55:35–42
- Bouaziz M, Leidig M, Gloaguen R (2011) Optimal parameter selection for qualitative regional erosion risk monitoring: a remote sensing study of SE Ethiopia. *Geosci Frontiers*. 2(2):237–245
- Chow V, Maidment D, Mays W (1988) Applied hydrology. McGRAW-HILL, New York
- De Jeng S (1999) Regional assessment of soil erosion using the distributed model SEMMED and remotely sensed data. *Catena* 37:291–308
- De Jong S (1994) Application of reflective remote sensing for land degradation studies. University of Utrecht
- De Steiguer J, Duberstein J, Lopes V (2003) The analytic hierarchy process as a means for integrated watershed management. In: Renard KG (ed) First interagency conference on research on the watersheds. Benson Arizona. 27–30 Oct 2003, 736–740
- Eswaran H, Lal R, Reich P (2001) Land degradation: an overview. In: Bridges EM, Hannam ID, Oldeman LR, Penning de Vries FWT, Scherr SJ, Sombatpanit S (eds) Response to land degradation. Sci Enfield, pp 20–35
- FAO (1989) Soil and water conservation in semi-arid areas. *FAO Soils Bulletin.*, 57. URL: <http://www.fao.org/docrep/T0321E/T0321E00.htm>
- Farhan Y, Nawaiseh S (2015) Spatial assessment of soil erosion risk using RUSLE and GIS techniques. *Environ Earth Sci* 74(6):4649–4669

- Ferro V, Giordano G, Lovino M (1991) Isoerosivity and erosion risk map for Sicily. *Hydrol Sci J* 36(6):549–564
- Gajbhiye S, Mishra S, Pandey A (2014) Prioritizing erosion-prone area through morphometric analysis: an RS and GIS perspective. *Appl Water Sci*. 4(1):51–61
- Garcia-Mozo HG, Galan C, Vazquez L (2006) The reliability of geostatic interpolation in olive field floral phenology. *Aerobiologia* 22(2):97–108
- Gitas I, Douros K, Minakou C, Silleos G, Karydas C (2009) Multi-temporal soil erosion risk assessment in N. Chalkidiki using a modified USLE raster model. *EARSeLeProceedings* 8(1):40–51
- Haan C, Barfield B, Hayes J (1994) Design hydrology and sedimentology for small catchments. Academic Press, San Diego
- Hickey R (2000) Slope angle and slope length solutions for GIS. *Cartography* 29:582–591
- Horton R (1932) Drainage basin characteristics. *Trans Am Geophys Union* 13(1):350–361
- Horton R (1945) Erosional development of streams and their drainage basins: hydrophysical approach to quantitative morphology. *Am bull Geol Soc*. 56:275–370
- Jaiswal R, Thomas T, Galkate R, Ghosh N, Singh S (2014) Watershed prioritization using saaty's AHP based decision support for soil conservation measures. *Water Resour Manage* 28(2):475–494
- Javed A, Khanday M, Ahmed R (2009) Prioritization of subwatersheds based on morphometric and land-use analysis using remote sensing and GIS techniques. *J Indian Soc Remote Sens*. 37:261–274
- Kachouri S, Achour H, Abida H, Bouaziz S (2014) Soil erosion hazard mapping using Analytic Hierarchy Process and logistic regression: a case study of Haffouz watershed, central Tunisia. *Arab J Geosci*. 8(6):4257–4268
- Kamaludin K, Lihan T, Ali Rahman Z, Mustapha M, Idris W, Rahim S (2013) Integration of remote sensing, RUSLE and GIS to model potential soil loss and sediment yield (SY). *Hydrol Earth Syst Sci* 10:4567–4596
- Kavian A, Fathollah Nejad Y, Habibnejad M, Soleimani K (2011) Modeling seasonal rainfall erosivity on a regional scale: a case study from Northeastern Iran. *Int J Environ Res* 5(4):939–950
- Kelarestaghi A, Jafarian Jeloudar Z (2011) Land use/cover change and driving force analyses in parts of northern Iran using RS and GIS techniques. *Arab J Geosci* 4:401–411
- Khan M, Gupta V, Moharana P (2001) Watershed prioritization using remote sensing and geographical information system: a case study from Guhiya. *India J Arid Environ* 49:465–475
- Kheir R, Cerdan O, Abdallah C (2006) Regional soil erosion risk mapping in Lebanon. *Geomorphology* 82(3–4):347–359
- Kim S-M, Choi Y, Suh J, Oh S, Park H-D, Yoon S-H (2012) Estimation of soil erosion and sediment yield from mine tailing dumps using GIS: a case study at the Samgwang mine, Korea. *Geosyst Eng* 15(1):2–9
- Kouli M, Soupios P, Valianatos F (2009) Soil erosion prediction using the Revised Universal Soil Loss Eq. (RUSLE) in a GIS framework, Chania, Northwestn Crete, Greece. *Environ Geol* 57(3): 483–497
- Kumar R, Kumar S, Lohani A, Nema R, Singh R (2000) Evaluation of geomorphological characteristics of a catchment using GIS. *GIS India*. 9(3):13–17
- Lal R (1998) Soil erosion impact on agronomic productivity and environment quality. *Crit Rev Plant Sci* 17(4):319–464
- Lal R (2001) Soil degradation by erosion. *Land Degrad Dev* 12(6):519–539
- Le Bissonnais Y, Montier C, Jamangne M, Daroussin J, King D (2001) Mapping erosion risk for cultivated soil in France. *Catena* 46(2–3):207–220
- Lee S (2004) Soil erosion assessment and its verification using the Universal Soil Loss Eq. and geographic information system: a case study at Boun, Korea. *Environ Geol* 45:457–465
- Lim JK, Sagong M, Engel B, Tang Z, Chio J, Kim K (2005) GIS-based sediment assessment tool. *Catena* 64(1):61–80
- Lin C, Lin W, Chou W (2002) Soil erosion prediction and sediment yield estimation: the Taiwan experience. *Soil Tillage Res*. 68:143–152
- Miller V (1953) A quantitative geomorphic study of drainage basin characteristics in the Clinch Mountain area, Virginia and Tennessee. Tech. Rep. 3 NR 389-402, Columbia University, Department of Geology, ONR, New York, NY, USA
- Morgan P (2005) Soil erosion and conservation. *Eur J Soil Sci*. 56(5):377–400
- Natural Resources Conservation Service Soil Survey Staff (1996) National soil survey handbook, title 430-VI. U.S. Government Printing Office, Washington
- Ni J, Li Y (2003) Approach to soil erosion assessment in terms of land-use structure changes. *J Soil Water Conserv* 58(3):158–169
- Nooka Ratnam K, Srivastava Y, Venkateshwara R, Amminedu E, Murthy K (2005) Check dam positioning by prioritization of micro-watersheds using SYI model and morphometric analysis—remote sensing and GIS perspective. *J Indian Soc Remote Sens* 33(1):25–38
- Parysow P, Wang G, Gertner G, Anderson A (2003) Spatial uncertainty analysis for mapping soil erodibility based on joint sequential simulation. *Catena* 53:65–78
- Pimentel D, Harvey C, Resosudarmo P, Sinclair K, Kurz D, McNair M, Blair R (1995) Environmental and economic costs of soil erosion and conservation benefits. *Science* 267:1117–1123
- Poesen J, Boardman J, Wilox B, Valentin C (1996) Water erosion monitoring and experimentation for global changes studies. *J Soil Water Conserv* 5:386–390
- Pradhan B, Chaudhari A, Adinarayana J, Buchroithner M (2011) Soil erosion assessment and its correlation with landslid events using remote sensing data and GIS. *Environ Monit Assess* 171:153–161
- Rahman M, Shi Z, Chongfa C (2009) Soil erosion hazard evaluation—an integrated use of remote sensing, GIS and statistical approaches with biophysical parameters towards management strategies. *Ecol Model* 220(13–14):1724–1734
- Renard K, Freimund J (1994) Using monthly precipitation data to estimate the R factor in the revised USLE. *J Hydrol* 157:287–306
- Renard, K., Foster, G., Weesies, G., McCool, D., & Yoder, D. (1997). Predicting soil erosion by water: A guide to conservation planning with the revised universal soil loss equation. U.S. Department of Agriculture, Agriculture Handbook 703, 384
- Saaty T (1986) Axiomatic foundation of analytical hierarchy process. *J Manage Sci* 31(7):841–855
- Sahin S, Kurum E (2002) Erosion risk analysis by GIS in environmental impact assessment: a case study: seyhan Kopru Dam conservation. *J Environ Manage* 66:239–249
- Schumms S (1956) Evolution of drainage systems and slopes in badlands at Perth Amboy, New Jersey. *Bull Geol Soc Am* 67:597–646
- Sharma J, Prasad J, Saha S, Pande L (2001) Watershed prioritization based on sediment yield index in eastern part of Don Valley using RS and GIS. *Indian J Soil Conserv* 29(1):7–13
- Shrimali S, Aggarwal S, Samra J (2001) Prioritizing erosion-prone areas in hills using remote sensing and GIS—a case study of the Sukhna lake catchment, northern India. *Int J App Earth Obs Geoinf* 3(1):54–60
- Strahler A (1964) Quantitative geomorphology of drainage basins and channel networks. In VT Chow (ed) Handbook of applied hydrology, pp 4–11
- Sun W, Shao Q, Liu J, Zhai J (2014) Assessing the effects of land use and topography on soil erosion on the Loess Plateau in China. *Catena* 121:151–163
- Terranova O, Antronico L, Coscarelli R, Iaquina P (2009) Soil erosion risk scenarios in the Mediterranean environment using

- RUSLE and GIS: an application model for Calabria (southern Italy). *Geomorphology* 112:228–245
- Van Remortel R, Maichle R, Hickey R (2004) Computing the LS Factor for the Revised Universal Soil Loss Eq. through array-based slope processing of digital elevation data using C++ executable. *Comput Geosci* 30:1043–1053
- Van Westen C (1997) Statistical landslide hazard analysis. ILWIS 2.1 for Windows application guide. ITC Publication Enschede, pp 73–84
- Vrieling A (2006) Satellite remote sensing for water erosion assessment: a review. *Catena* 65:2–18
- Wang G, Wentz S, Gertner G, Anderson A (2002) Improvement in mapping vegetation cover factor for the universal soil loss Eq. by geostatistical methods with Landsat Thematic Mapper images. *Int J Remote Sens* 23:3649–3667
- Wischmeier W, Smith D (1978) Predicting rainfall erosion. Losses: a guide to conservation planning. *Agriculture Handbook*, US Department of Agriculture, Washington, DC 537: 58
- Wischmeier W, Johnson C, Cross B (1971) A soil erodibility nomograph for farmland and construction sites. *J Soil Water Conserv* 26:189–193
- Yoshino K, Ishioka Y (2005) Guidelines for soil conservation towards integrated basin management for sustainable development: a new approach based on the assessment of soil loss risk using remote sensing and GIS. *J. Water Environ.* 3(4):235–247
- Zhang Y, Degroote J, Wolter C, Sugumaran R (2009) Integration of Modified Universal Soil Loss Eq. (MUSLE) into a GIS framework to assess soil erosion risk. *Land Degrad Dev* 20(1):84–91
- Zhang X, Wu B, Ling F, Zeng Y, Yan N, Youan C (2010) Identification of priority areas for controlling soil erosion. *Catena*. 83:76–86